

***SRG* /ART-XC discovery of pulsations from RX J0535.0-6700: another X-ray pulsar in the LMC**

I. A. Mereminskiy^{1*}, A. S. Gorban^{1,2}, Yu. S. Klein^{2,1}, E. A. Ushakova^{2,1}, A. N. Semena¹,
A. A. Lutovinov¹, A. Yu. Tkachenko¹, S. V. Molkov¹

¹*Space Research Institute, Russian Academy of Sciences, Profsoyuznaya str., 84/32, 117997, Moscow, Russia*

²*National Research University 'Higher School of Economics', Pokrovsky bulvar, 11, 109028, Moscow, Russia*

Received 01.04.2025. Revised 07.04.2025. Accepted 07.04.2025.

Abstract — Using the *Mikhail Pavlinsky* ART-XC onboard the *SRG* observatory we have detected, for the first time, X-ray pulsations with a period of ≈ 106 s from the poorly-studied high-mass X-ray binary RX J0535.0-6700 located in the Large Magellanic Cloud (LMC), thus proving that the accretor is a neutron star with strong magnetic field. Pulsations with similar period were also found in archival archival data from *Chandra* and *XMM-Newton* telescopes. Using photometry from *WISE* we shown that the source demonstrate significant variability in IR during the last twenty years, which could be caused by a secular evolution of the decretion disk. This discovery makes RX J0535.0-6700 another member of the large family of X-ray pulsars with Be-type companions in the LMC.

Key words: *X-rays: individuals: RX J0535.0-6700, X-rays: binaries, accretion, accretion disks*

INTRODUCTION

The Large Magellanic Cloud (LMC) is a satellite dwarf galaxy of the Milky Way. Due to a powerful star formation outbursts in the recent past ($\approx 10^7$ years ago, see, e.g. Shtykovskiy & Gilfanov 2005; Antoniou & Zezas 2016) it now harbours a large population of bright high-mass X-ray binaries (HMXBs). This population is very convenient to study with the modern X-ray telescopes due to a well-determined distance to LMC (49.6 kpc, Pietrzyński et al., 2019) and a moderate line-of-sight extinction (Staveley-Smith et al., 2003).

However, the duty cycle of such systems is quite low, about 10% or even less (Sidoli & Paizis, 2018; Kennea et al., 2018) and major part of the time they reside in a low state with X-ray luminosity of $L_X \lesssim 10^{34}$ erg s⁻¹. Even for the most sensitive modern X-ray telescopes this makes them hard to study with observations of sensible exposures (dozens of ks). Therefore, in order to study these sources better, e.g. to measure neutron stars spin period, multiple observations are required, allowing one to catch new or known sources in an outburst.

RX J0535.0-6700 was discovered by the *ROSAT* observatory (Truemper, 1982) during the extensive LMC survey, composed from more than 200 observations performed from 1990 to 1994 (Haberl & Pietsch, 1999). The source was detected at the luminosity of $\approx 3 \times 10^{35}$

erg s⁻¹. Haberl & Pietsch (1999) suggested that the optical counterpart of RX J0535.0-6700 is the bright blue star GRV 0535-6702, which was earlier classified as a Mira-type variable, given its flux variations with a period of 241 days (Reid et al., 1988). Later, Negueruela & Coe (2002) performed optical spectroscopy of the candidate star and classified it as B0 Ve star, thus making RX J0535.0-6700 another Be-X-ray binary (BeXRB, Riquelme et al. 2012). In such systems a neutron star (NS) accretes matter from a decretion disc of the Be-star (see, Belczynski & Ziolkowski, 2009). Depending on orbital parameters an accretion could be either quasi-persistent (Pfahl et al., 2002) or transient ones, with powerful outbursts occurring once per orbit or more rarely (see, e.g., Okazaki & Negueruela, 2001).

Using data from the *NTT* telescope Riquelme et al. (2012) measured the total equivalent width of the H_α line from the decretion disk in RX J0535.0-6700 to be -7.9\AA . Based on the $P_{orb} - EW(H_\alpha)$ relation of BeXRBs (Reig, 2011) and assuming that the orbital period of RX J0535.0-6700 is $P_{orb} \approx 241$ days one can suggest that the decretion disk was far from its maximal size during the *NTT* observation in 2004.

In 2024 RX J0535.0-6700 was serendipitously observed by the *Mikhail Pavlinsky* ART-XC telescope (Pavlinsky et al., 2021) onboard the *SRG* observatory (Sunyaev et al., 2021) during long pointing observations of the another enigmatic LMC source 1A 0538-

* e-mail: i.a.mereminskiy@gmail.com

Table 1. List of X-ray observations of RX J0535.0-6700

ObsID	Start time, MJD	Exposure, ks
ART-XC		
124101290010	60464.86	173
124101290020	60498.12	260
124101290030	60508.20	86
XMM-Newton		
0071740501	52373.84	24
Chandra		
27078	59948.23	25
27077	60147.66	28
26555	60201.30	31
28907	60536.70	18

66. These data allowed us to detect for the first time coherent pulsations with a period of $\simeq 106$ s from the source. We identified this period as a spin period of the magnetic neutron star, thereby confirming classification of RX J0535.0-6700 as BeXRB. We have also looked through archival X-ray observations by the *Chandra* and XMM-Newton to trace the evolution of the spin-period and to study the source spectrum and its variability over the long timescales.

OBSERVATIONS AND DATA ANALYSIS

The RX J0535.0-6700 happened to be located inside the ART-XC field of view during monitoring observations of X-ray pulsar 1A 0538-66 in the summer of 2024. Three long observations were carried out: first one in the beginning of June and two others in July (see Tab. 1 for details). In all three observations the source was detected at a significance level $> 10\sigma$ in the standard 4 – 12 keV band.

The ART-XC data was processed with the standard pipeline ARTPRODUCTS v0.9 using calibration data version CALDB 20230228. For a temporal analysis we applied barycentric corrections to photon arrival times and extracted event lists and light curves for each observation from circular aperture with $1'$ radius, centred on the source position. The spectra were extracted from the smaller region with radius of $R = 45''$. The background spectrum was obtained from earlier observations of a blank fields, and was normalized by the count rate at energies above 60 keV, where the effective area of the mirror system is negligible. Such approach allows to accumulate background spectra with better statistics and diminish the differences in response of individual detector pixels. The data from all seven telescope modules were combined for spectral and temporal analysis.

We also decided to look through the available archival data on the source, in order to trace its long-term behaviour. RX J0535.0-6700 was observed by

the XMM-Newton observatory (Jansen et al., 2001) in 2002. Unfortunately, due to the observation mode, the source was observed only by the MOS1 and MOS2 cameras. It was located in outer chips, which operated in the standard imaging mode, thus limiting temporal resolution to the frame integration time of 2.6 s. After standard data reprocessing using XMM-SAS v20, we extracted event lists and spectra from the circular apertures of $R = 22.5''$ ($R = 20''$) for MOS1 (MOS2). The background spectra were extracted from the empty areas of the field on the same camera chips.

This part of LMC also was extensively covered with *Chandra* (Weisskopf et al., 2000) observations in 2023-2024. We selected four observations in which RX J0535.0-6700 was inside the telescope field of view and reprocessed data using CIAO 4.17 (Fruscione et al., 2006). Then we examined sky images in the *Chandra* broad band (0.5-7 keV). As it turned out, the source was securely detected in all of them, although it was the brightest in the last one, which was performed in 2024, nearly a month after the latest ART-XC observation. In this observation *Chandra* accumulated about 1600 photons from the source, enabling to perform detailed spectral and temporal analysis. For each observation we extracted spectrum from a circular aperture with $R = 6''$ centered on the source position; the background spectrum was obtained from empty parts of the field on the same CCD. For the last observation we have also extracted source lightcurve from the same circular aperture. Unfortunately, similar to XMM-Newton, the temporal resolution for these data is also limited by the frame integration time, which is 3.1s.

For spectral modelling we used the XSPEC v12.12.1 package (Arnaud et al., 1999). Given the low counting statistics we rebinned all spectra in order to have at least 5 counts per bin and applied W-statistics (Wachter et al., 1979) for fitting. Uncertainties on model parameters were derived by means of long Markov chains. To estimate a quality of best-fit models we employed the Cramér-von Mises statistics; for each model 1000 simulated datasets were produced, then for each dataset test statistic was calculated. A fraction of datasets with the lower (i.e. better) test statistic than for real data shows how well the model corresponds to the observed spectrum. For valid models this ratio should be about 50%. For all models, presented below, this ratio is below 60%, indicating that this models are acceptable.

TIMING ANALYSIS

Pulsations

Upon the identification of the observed source with the BeXRB candidate it became clear that ART-XC

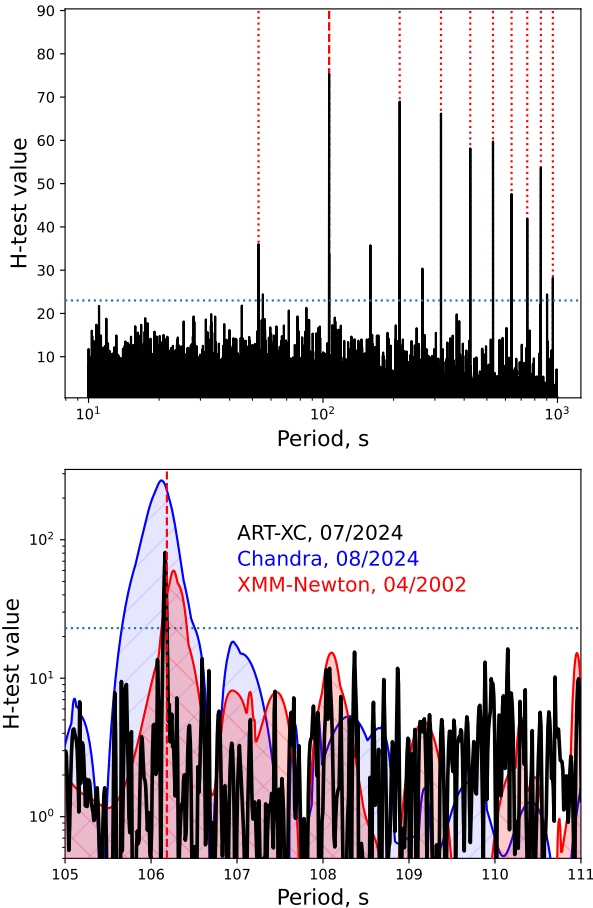


Fig. 1. *Upper panel:* H-test periodogram of the first ART-XC observation (4-10 keV). Vertical red dashed line shows the fundamental period of the NS rotation, dotted lines shows harmonics and subharmonic. *Lower panel:* part of the periodogram around the fundamental period from the second ART-XC observation (4-10 keV, black), XMM-Newton (0.2-10 keV, red) and Chandra (0.5-10 keV, blue) observations.

data could be used to search for the coherent pulsations from the source. From the event lists in the 4-10 keV band we calculated H-test (Hart, 1985) periodograms, utilising up to 20 harmonics (Buccheri et al., 1983). The periodogram constructed on logarithmic grid of 4×10^4 test periods from 10 to 1000 s is shown in Fig. 1. A horizontal line at $H = 23$ corresponds to the detection of pulsations at a significance level of > 0.9999 . The peak at $P_s \approx 106$ s clearly stands out, along with its harmonics ($P = 0.5P_s, 1.5P_s, 2P_s, 2.5P_s, 3P_s$ etc.). We identified this period as the spin period of neutron star in RX J0535.0-6700.

In a similar way we have produced periodograms for XMM-Newton and Chandra data. For each photon we generated a mock-up arrival time with a uniform random distribution inside the frame length. As it could be seen from the lower panel of Fig. 1 the pulsations with a nearly same period are detected in both datasets. Pulsations are also present in the second ART-XC observation, which was performed nearly a month after the first one. No periodic signal is detected at similar significance threshold in the third ART-XC observation.

Although the periodogram is a reliable method to search for coherent signals in data, in order to study properties of such signals (e.g., exact measuring of the pulse period, pulse profiles) it is convenient to employ other methods.

Period determination and pulse profile

In order to measure the spin period during each observation we constructed the 4-10 keV ART-XC lightcurves with the resolution of 1 s and used the epoch folding method (Leahy et al., 1983). Given the low count statistic (an observed ART-XC count rate is about 400 counts per day) to estimate uncertainty of the period measurement we used the technique, similar to one used by Mereminskiy et al. (2022): assuming that both background and mean over period source count rates were constant through the observation and using a piece-wise constant representation of the observed pulse profile we produced 1000 simulated lightcurves, that matches in the length and coverage with the real one. Then, for each simulated lightcurve we found the best period using the same epoch folding method. Boundaries of a confidence interval for the actual measurement was then calculated as 16% and 84% quantiles of sample of periods from simulated lightcurves. Applying this technique to the ART-XC data we obtained period measurements of $P = 106.180^{+0.003}_{-0.005}$ s (68% confidence interval) and $P = 106.160 \pm 0.004$ s for first two observations, correspondingly.

The pulse profile measured in the second ART-XC

observation is shown in Fig. 2 (upper panel). Formally, it has a simple one-peaked shape, but fine details could be lost due to insufficient statistics.

For *Chandra* and XMM-*Newton* observations we used same technique, taking into account the corresponding frame accumulation times (3.1 and 2.6 s, correspondingly). For each event list we have produced 1000 realisations, assigning random arrival times inside the frame for each photon. Then we found best-fit period for each realisation. Using the median and corresponding quantiles of sample of periods for each dataset, we derived $P = 106.26^{+0.02}_{-0.02}$ s for the XMM-*Newton* observation in 2002 and $P = 106.12 \pm 0.01$ s for the last *Chandra* observation in 2024. Corresponding pulse profiles from these datasets are shown in Fig. 2 (middle and bottom panels).

It is interesting to note that the pulsed fraction measured for all profiles is quite high: $\approx 60\%$ for ART-XC and XMM-*Newton* and even higher $\approx 70\%$ for *Chandra* data in narrow (0.5-2 and 2-10 keV) bands.

SPECTRAL ANALYSIS

In order to derive the source luminosity in our observations we investigated its X-ray spectra.

Given the relatively low photons statistics we chose to use a simple phenomenological model consisting of the intrinsic X-ray continuum described by a cut-off powerlaw and two absorption components – one due to the local absorption near the source and another one that corresponds to the line-of-sight absorption in the Milky Way: `tbabs*tbfeo*cutoffpl` in XSPEC terms. The thickness of the neutral hydrogen in the Galaxy in the source direction was fixed at the value of $N_{\text{H,loc}} = 10^{21} \text{ cm}^{-2}$ (HI4PI Collaboration et al., 2016). Since the LMC metallicity significantly differs from the Solar one, following Ducci et al. (2019) for the local absorption we used oxygen and iron abundances of 0.33 and 0.38, respectively.

Despite the model simplicity, it is not trivial to robustly estimate its parameters from a narrow-band spectrum due to arising degeneracies. Therefore we decided to simultaneously fit spectra from first two ART-XC observations and *Chandra* spectrum, which was obtained nearly a month later. Two ART-XC spectra are similar in shape, and observed 4-12 keV count rates differs by less than 10%. However, during the *Chandra* observation the source was significantly brighter. To account for a differences in normalization we added multiplicative constant to the model. The resulting broadband X-ray spectrum (0.8-16 keV) is shown in Fig. 3 by red and black crosses. Thanks to its extended coverage we were able to measure an intrinsic absorption of $N_{\text{H,loc}} = 2.8^{+7.5}_{-2.1} \times 10^{21} \text{ cm}^{-2}$ (hereafter uncertainties on parameters corresponds to 90%

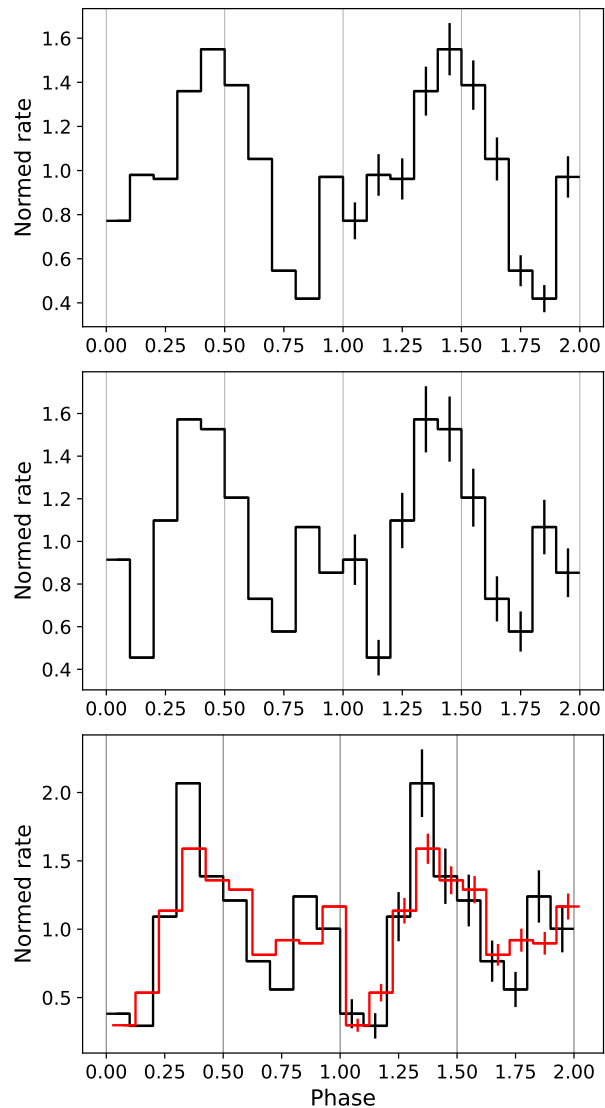


Fig. 2. Pulse profile observed during different epochs. *Upper panel:* ART-XC, 4-10 keV, *middle:* XMM-*Newton*, 0.5-10 keV, *lower:* *Chandra* 0.5-2 keV (black) and 2-10 keV (red).

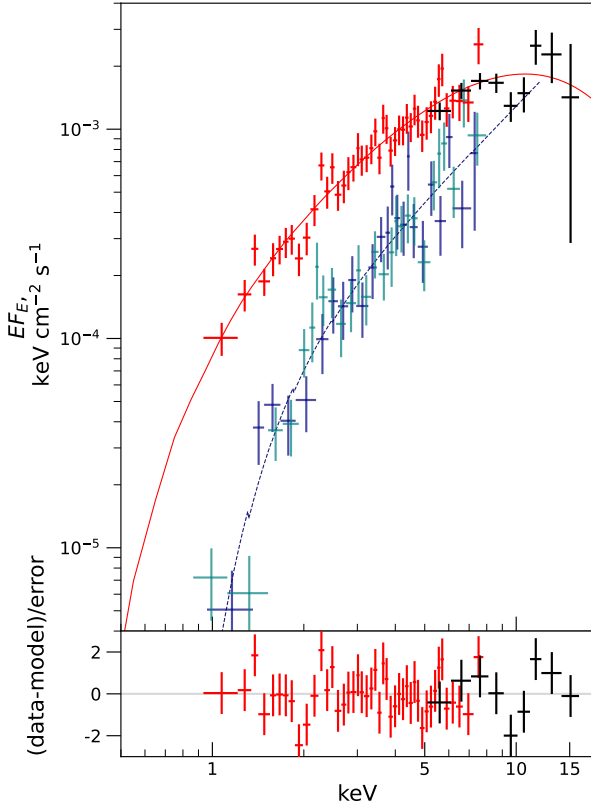


Fig. 3. X-ray spectra obtained in 2024 by *Chandra* (red crosses) and ART-XC (black crosses, scaled to match *Chandra* data), shown along with the best-fit model (solid line) and corresponding residuals. Navy and cyan points shows the spectrum from XMM-*Newton* MOS1/MOS2, accumulated in 2002.

level), a power-law slope of $\Gamma = 0.23^{+0.52}_{-0.17}$ and a cut-off energy of $E_{\text{cut}} = 6.0^{+7.2}_{-1.2}$ keV.

We used these parameters to estimate a bolometric 0.1–30 keV luminosity for all ART-XC and *Chandra* observations in 2023–2024. As it is shown in Fig. 4, over two years the source have brightened from 4×10^{34} erg s $^{-1}$ up to 2×10^{36} erg s $^{-1}$, although the growth was not monotonic, with an apparent variability on timescales of weeks.

Interestingly, while the archival spectrum from the 2002 XMM-*Newton* observation could be described with the similar spectral model with the intrinsic absorption fixed at $N_{\text{H,loc}} = 2.8 \times 10^{21}$ cm $^{-2}$ it leads to unphysical continuum parameters, such as the extremely hard power-law slope of $\Gamma \lesssim -1.5$ and low cut-off energy $E_{\text{cut}} \approx 3$ keV. The spectrum could also be described with a single blackbody model with the temperature of $kT \approx 2$ keV and characteristic size of the emission region of $R \approx 500$ m. In this case the total luminosity turns out to be around 3×10^{35} erg s $^{-1}$. Note that such hotspots are often observed in X-ray pulsars, albeit at much higher luminosities – typically above 10^{37}

erg s $^{-1}$ (Mushtukov & Tsygankov, 2022).

However, by allowing a local absorption to vary freely we obtained a satisfactory fit with a moderate power-law index $\Gamma = 0.49^{+0.47}_{-0.25}$ and much larger $N_{\text{H,loc}} = 23.5^{+17.0}_{-7.1} \times 10^{21}$ cm $^{-2}$. The spectral coverage is not enough to constrain the cut-off energy. This model, along with the unfolded MOS1/MOS2 data, shown in Fig. 3 by a navy line and navy and cyan crosses. It is impossible to get a meaningful estimate of the bolometric luminosity for such a hard spectrum. But using the soft X-ray luminosity of $L_{0.1-10\text{keV}} \approx 4 \times 10^{35}$ erg s $^{-1}$ and assuming that a bolometric correction factor is moderate ($L_{0.1-30\text{keV}}/L_{0.1-10\text{keV}} \approx 1.7$ for a broadband ART-XC/*Chandra* spectrum) one can guess that the total bolometric luminosity was about 10^{36} erg s $^{-1}$ at the moment of the XMM-*Newton* observation in 2002.

It is interesting to note that XMM-*Newton* observed the field of RX J0535.0-6700 several times on May – June, 2018, but the source was not detected. We queried the XMM-*Newton* Science Archive upper limit server (Ruiz et al., 2022) and found that a typical 2σ upper limit on the source flux is $\approx 3 \times 10^{-14}$ erg cm $^{-2}$ s $^{-1}$ in the 0.2–12 keV energy range. This value corresponds to the intrinsic luminosity of $\approx 10^{34}$ erg s $^{-1}$, assuming that the spectral shape was similar to the one observed in 2024.

DISCUSSION

The long-term variability of the X-ray luminosity in Be-systems, such as observed in RX J0535.0-6700, could be related to the secular evolution of the decretion disk (Wisniewski et al., 2010). We examined the publicly available data from the IR space telescope *WISE* (Wright et al., 2010; Mainzer et al., 2014) to search for the presence of a characteristic “brighter-redder” variability, which is related to variations of the decretion disk size. Light curves in filters W1 and W2 are shown in Fig. 4. Unfortunately, amount of the W2 data is not enough for definitive conclusions about the state of the decretion disk in 2023–2024. But it could be seen, that the brightness in the W2 filter has grown from 14.5 to 13 magnitude since 2010; additionally the W1 magnitude was also decreased by ≈ 1 mag. Also, there is an apparent change in the variability pattern around 2019. Further spectroscopic observations are necessary to probe the decretion disk state in this system.

If the optical period of 241 days (Reid et al., 1988) is indeed the orbital one, then a detected spin-period of $P \approx 106$ s puts RX J0535.0-6700 on a region of the Corbet diagram (Corbet, 1986) occupied by other BeXRBs (see, updated versions of the diagram in Grebenev, 2010; Kretschmar et al., 2019).

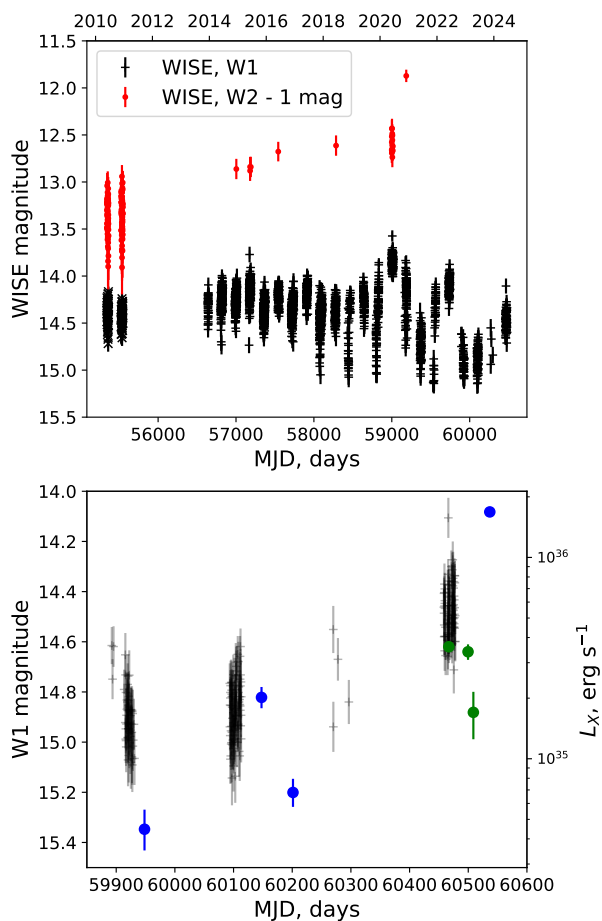


Fig. 4. *Upper panel:* 2010-2024 IR lightcurve of RX J0535.0-6700 in WISE W1 (shown in black) and W2 (red, shifted by 1 mag) filters.

Lower panel: zoom-in on 2023-2024 WISE W1 data. X-ray luminosities of RX J0535.0-6700 from ART-XC and *Chandra* observations shown with green and blue circles, correspondingly.

The stability of the observed NS spin-period over the last twenty years implies that it is close to the equilibrium one. Assuming that the mean mass accretion rate in RX J0535.0-6700 is $\langle \dot{M} \rangle \approx 2 \times 10^{-11} M_{\odot} \text{ yr}^{-1}$, which corresponds to mean luminosity of $\langle L_X \rangle \approx 10^{35} \text{ erg s}^{-1}$, one could estimate the NS magnetic field strength using Eq. 9 from Bildsten et al. 1997: $B \approx 5 \times 10^{12} \text{ G}$. This is not enough for the “propeller” effect (Illarionov & Sunyaev, 1975) to set on, allowing the accretion to take place through a cold disk (Tsygankov et al., 2017). This could explain a long lasting episode with low luminosity ($L_X \approx 3 \times 10^{35} \text{ erg s}^{-1}$) observed by ART-XC, which is not typical for a BeXRB variability.

CONCLUSION

We have discovered coherent X-ray pulsations with a period of 106.2 s from RX J0535.0-6700 – a BeXRB located in the LMC. Pulsations present in the ART-XC data, in which they were revealed initially, as well as in XMM-*Newton* and *Chandra* data, obtained during different epochs. The pulse period remains relatively stable in all observations, spanning more than 20 years, and the pulsed fraction is quite high also in all observations, above 50% in all energy bands.

The source X-ray spectrum is typical for accreting X-ray pulsars and can be described by an absorbed power law with an exponential cutoff. It seems that the local absorption has changed dramatically between 2002 and 2024, although it should be mentioned that the accurate measurement of $N_{\text{H,loc}}$ in the standard X-ray band (0.5-10 keV) is complicated. The broadband observations are required to better characterize spectral parameters.

The optical companion of RX J0535.0-6700 B0Ve star exhibits a strong variability in the IR bands, which could indicate the secular variations of the accretion disk.

Finally we can conclude that all obtained data confirms that RX J0535.0-6700 is the 28th member of a large family of BeXRBs with neutron stars in the LMC (Haberl et al., 2023).

This work is based on observations with the Mikhail Pavlinsky ART-XC telescope, hard X-ray instrument on board the SRG observatory. The SRG observatory was created by Roskosmos in the interests of the Russian Academy of Sciences represented by its Space Research Institute (IKI) in the framework of the Russian Federal Space Program, with the participation of Germany. The ART-XC team thanks Lavochkin Association (NPOL) with partners for the creation and operation of the SRG spacecraft (Navigator)

This research has made use of data obtained from the Chandra Data Archive provided by the Chandra X-ray Center (CXC).

Research is partially based on observations obtained with XMM-Newton, an ESA science mission with instruments and contributions directly funded by ESA Member States and NASA

This work was supported by the Minobrnauki RF grant 075-15-2024-647.

REFERENCES

1. Antoniou V., Zezas A., 2016, *Mon. Not. R. Astron. Soc.*, 459, 528
2. Arnaud K., Dorman B., Gordon C., 1999, XSPEC: An X-ray spectral fitting package, *Astrophysics Source Code Library*, record ascl:9910.005
3. Belczynski K., Ziolkowski J., 2009, *Astrophys. J.*, 707, 870
4. Bildsten L., et al., 1997, *Astrophys. J. Suppl. Ser.*, 113, 367
5. Bucccheri R., et al., 1983, *Astron. Astrophys.*, 128, 245
6. Corbet R. H. D., 1986, *Mon. Not. R. Astron. Soc.*, 220, 1047
7. Ducci L., Mereghetti S., Santangelo A., 2019, *The Astrophysical Journal Letters*, 881, L17
8. Fruscione A., et al., 2006, in Silva D. R., Doxsey R. E., eds, *Society of Photo-Optical Instrumentation Engineers (SPIE) Conference Series Vol. 6270, Observatory Operations: Strategies, Processes, and Systems*. p. 62701V, doi:10.1117/12.671760
9. Grebenev S. A., 2010, *arXiv e-prints*, p. arXiv:1004.0293
10. HI4PI Collaboration et al., 2016, *Astron. Astrophys.*, 594, A116
11. Haberl F., Pietsch W., 1999, *Astron. Astrophys.*, 344, 521
12. Haberl F., et al., 2023, *Astronomy & Astrophysics*, 671, A90
13. Hart J. D., 1985, *Journal of Statistical Computation and Simulation*, 21, 95
14. Illarionov A. F., Sunyaev R. A., 1975, *Astron. Astrophys.*, 39, 185
15. Jansen F., et al., 2001, *Astron. Astrophys.*, 365, L1
16. Kennea J. A., Coe M. J., Evans P. A., Waters J., Jasko R. E., 2018, *Astrophys. J.*, 868, 47
17. Kretschmar P., et al., 2019, *New Astron. Rev.*, 86, 101546
18. Leahy D. A., Darbro W., Elsner R. F., Weisskopf M. C., Sutherland P. G., Kahn S., Grindlay J. E., 1983, *Astrophys. J.*, 266, 160
19. Mainzer A., et al., 2014, *Astrophys. J.*, 792, 30
20. Mereminskiy I. A., Mushtukov A. A., Lutovinov A. A., Tsygankov S. S., Semena A. N., Molkov S. V., Shtykovsky A. E., 2022, *Astron. Astrophys.*, 661, A33
21. Mushtukov A., Tsygankov S., 2022, *arXiv e-prints*, p. arXiv:2204.14185
22. Negueruela I., Coe M. J., 2002, *Astron. Astrophys.*, 385, 517
23. Okazaki A. T., Negueruela I., 2001, *Astron. Astrophys.*, 377, 161
24. Pavlinsky M., et al., 2021, *Astron. Astrophys.*, 650, A42
25. Pfahl E., Rappaport S., Podsiadlowski P., Spruit H., 2002, *Astrophys. J.*, 574, 364
26. Pietrzyński G., et al., 2019, *Nature*, 567, 200
27. Reid N., Glass I. S., Catchpole R. M., 1988, *Mon. Not. R. Astron. Soc.*, 232, 53
28. Reig P., 2011, *Ap&SS*, 332, 1
29. Riquelme M. S., Torrejón J. M., Negueruela I., 2012, *Astron. Astrophys.*, 539, A114
30. Ruiz A., Georgakakis A., Gerakakis S., Saxton R., Kretschmar P., Akylas A., Georgantopoulos I., 2022, *Mon. Not. R. Astron. Soc.*, 511, 4265
31. Shtykovskiy P., Gilfanov M., 2005, *Astron. Astrophys.*, 431, 597
32. Sidoli L., Paizis A., 2018, *Mon. Not. R. Astron. Soc.*, 481, 2779
33. Staveley-Smith L., Kim S., Calabretta M. R., Haynes R. F., Kesteven M. J., 2003, *Mon. Not. R. Astron. Soc.*, 339, 87
34. Sunyaev R., et al., 2021, *Astron. Astrophys.*, 656, A132
35. Truemper J., 1982, *Advances in Space Research*, 2, 241
36. Tsygankov S. S., Mushtukov A. A., Suleimanov V. F., Doroshenko V., Abolmasov P. K., Lutovinov A. A., Poutanen J., 2017, *Astron. Astrophys.*, 608, A17
37. Wachter K., Leach R., Kellogg E., 1979, *Astrophys. J.*, 230, 274
38. Weisskopf M. C., Tananbaum H. D., Van Speybroeck L. P., O'Dell S. L., 2000, *Chandra X-ray Observatory (CXO): overview*. pp 2–16, doi:10.1117/12.391545
39. Wisniewski J. P., Draper Z. H., Bjorkman K. S., Meade M. R., Bjorkman J. E., Kowalski A. F., 2010, *Astrophys. J.*, 709, 1306
40. Wright E. L., et al., 2010, *Astron. J.*, 140, 1868